Quality of epitaxial InAs nanowires controlled by catalyst size in molecular beam epitaxy

Zhi Zhang, Zhen-Yu Lu, Ping-Ping Chen, Hong-Yi Xu, Ya-Nan Guo, Zhi-Ming Liao, Sui-Xing Shi, Wei Lu, and Jin Zou

Citation: Applied Physics Letters **103**, 073109 (2013); doi: 10.1063/1.4818682
View online: http://dx.doi.org/10.1063/1.4818682
View Table of Contents: http://scitation.aip.org/content/aip/journal/apl/103/7?ver=pdfcov
Published by the AIP Publishing

Articles you may be interested in

Polarity driven simultaneous growth of free-standing and lateral GaAsP epitaxial nanowires on GaAs (001) substrate
Appl. Phys. Lett. **103**, 223104 (2013); 10.1063/1.4834377

Inhomogeneous Si-doping of gold-seeded InAs nanowires grown by molecular beam epitaxy
Appl. Phys. Lett. **102**, 223105 (2013); 10.1063/1.4809576

Au impact on GaAs epitaxial growth on GaAs (111)B substrates in molecular beam epitaxy
Appl. Phys. Lett. **102**, 063106 (2013); 10.1063/1.4792053

Growth kinetics in position-controlled and catalyst-free InAs nanowire arrays on Si(111) grown by selective area molecular beam epitaxy
J. Appl. Phys. **108**, 114316 (2010); 10.1063/1.3525610

ZnTe nanowires grown on GaAs(100) substrates by molecular beam epitaxy
Appl. Phys. Lett. **89**, 133114 (2006); 10.1063/1.2357334

This article is copyrighted as indicated in the article. Reuse of AIP content is subject to the terms at: http://scitation.aip.org/termsconditions. Downloaded to IP: 130.56.107.194 On: Fri, 04 Apr 2014 13:51:33

Quality of epitaxial InAs nanowires controlled by catalyst size in molecular beam epitaxy

Zhi Zhang,[1] Zhen-Yu Lu,[2] Ping-Ping Chen,[2] Hong-Yi Xu,[1] Ya-Nan Guo,[1] Zhi-Ming Liao,[1] Sui-Xing Shi,[2] Wei Lu,[2] and Jin Zou[1,3,a)]

[1]*Materials Engineering, The University of Queensland, St. Lucia, Queensland 4072, Australia*
[2]*National Laboratory for Infrared Physics, Shanghai Institute of Technical Physics, Chinese Academy of Sciences, 500 Yu-Tian Road, Shanghai 200083, People's Republic of China*
[3]*Centre for Microscopy and Microanalysis, The University of Queensland, St. Lucia, Queensland 4072, Australia*

(Received 29 May 2013; accepted 2 August 2013; published online 13 August 2013)

In this study, the structural quality of Au-catalyzed InAs nanowires grown by molecular beam epitaxy is investigated. Through detailed electron microscopy characterizations and analysis of binary Au-In phase diagram, it is found that defect-free InAs nanowires can be induced by smaller catalysts with a high In concentration, while comparatively larger catalysts containing less In induce defected InAs nanowires. This study indicates that the structural quality of InAs nanowires can be controlled by the size of Au catalysts when other growth conditions remain as constants. © *2013 AIP Publishing LLC*. [http://dx.doi.org/10.1063/1.4818682]

III–V semiconductor nanowires have attracted extensive attentions in the recent decades due to their distinct physical properties and hence potential applications in nanoelectronics and optoelectronics.[1,2] Currently, the most typical approach for nanowire growth is the vapor-liquid-solid (VLS)[3] mechanism, in which reactant from ambient vapor is incorporated into metallic catalyst nanoparticles to form liquid droplets, and the supersaturation of reactant atoms leads to anisotropic nanowire growth. Metal-catalyzed nanowire growth under the eutectic temperature via the VLS process has also been reported, and the existence of liquid droplets is attributed to the undercooling of nanodroplets and nanoscale size effect.[4,5]

As a key III–V semiconductor, InAs has attracted special research interest due to its very high electron mobility,[6] low-resistance ohmic contact,[7] narrow band gap, and small electron effective mass.[8] The combination of these unique features and the distinct characteristics of nanowires have made InAs nanowires a promising candidate for applications in single-electron transistors,[9] the Josephon junctions,[10] resonant tunnelling diodes,[11] and ballistic transistors.[12,13]

For nanowires to be practically useful, minimizing the lattice defects in nanowires has been a challenging task. In this regard, several strategies have been implemented. For example, it has been demonstrated that structural quality of III–V nanowires can be well controlled by tuning growth parameters, such as V/III ratio and/or growth temperature.[14] On the other hand, theoretical predictions has indicated that nanowire diameter[15] and catalyst supersaturation[16,17] can greatly influence the crystal structure of III–V nanowires and their qualities. The effect of nanowire diameters on the structural transition of wurtzite and zinc-blende structures in InAs nanowires grown by metal-organic chemical vapor deposition has been demonstrated.[18] However, understanding the size-dependent growth of InAs nanowires and achieving high-quality InAs nanowires require further investigations.[19]

In this letter, we investigated the structural characteristics of Au-catalyzed epitaxial InAs nanowires grown by molecular beam epitaxy (MBE). Through detailed structural and chemical characterizations using electron microscopy, it has been found that the structural quality of InAs nanowires can be well controlled by the size of Au catalysts. The physical reason behind these observed experimental results is explored.

The InAs nanowires were grown in a Riber 32 MBE system using Au-assisted growth mode on a GaAs $\{111\}_B$ substrate. The substrate surface was first degassed in the preparation chamber for 15 min at 250 °C. Then the substrate was transferred to the growth chamber to be thermally deoxidized at 610 °C, and a ~200 nm thick GaAs buffer layer was grown on the GaAs $\{111\}_B$ substrate at 580 °C to achieve atomically flat surface. After that, the substrate was transferred back to the preparation chamber, and a thin Au film was then deposited on the top of the GaAs buffer layer by the vacuum thermal evaporation. The Au-coated GaAs substrate was then transferred back to the MBE growth chamber and annealed at 500 °C for 5 min under As ambient to agglomerate the Au thin film into nanoparticles via Oswald ripening. This thin film generated Au nanoparticles is a simple and cost efficient approach.[20,21] After the annealing, the substrate temperature was lowered to 430 °C, and the In source was introduced to initiate InAs nanowires growth for 100 min with a V/III ratio of 20.

The morphological characteristics of grown InAs nanowires were investigated by scanning electron microscopy (SEM, JEOL 7800F, operated at 10 kV), and their detailed structural and chemical characteristics were investigated by transmission electron microscopy [TEM, Philips Tecnai F20, operated at 200 kV, equipped with X-ray energy dispersive spectroscopy (EDS) for compositional analysis, and Philips Tecnai F30]. Individual nanowires for TEM analysis were prepared by ultrasonicating the nanowire samples in ethanol and then dispersing nanowires onto holey carbon films supported by Cu grids.

a)Email: j.zou@uq.edu.au

 © 2013 AIP Publishing LLC

This article is copyrighted as indicated in the article. Reuse of AIP content is subject to the terms at: http://scitation.aip.org/termsconditions. Downloaded to IP: 130.56.107.194 On: Fri, 04 Apr 2014 13:51:33

Figure 1 is a typical tilted SEM image and shows that the majority nanowires are vertically grown on the substrate. As can be seen, the heights of these nanowires vary, similar to our early observation of InAs nanowires grown on the GaAs substrate.[22] It should be noted that these nanowires have diverse diameters, as illustrated in the inset. Based on the nanowire morphology, no tapering was observed, although tapering, caused by lateral growth of nanowires,[23] often exists in epitaxially grown nanowires.

To understand the structural and chemical characteristics of grown nanowires, detailed TEM investigations were performed. Figure 2(a) is a bright-field TEM image of a typical thick InAs nanowire and shows uniform diameter (~45 nm) along axial direction of the nanowire. Figure 2(b) is a high-resolution TEM image of the nanowire section near the catalyst, in which the nanowire has the wurtzite structure with many planar defects along its axial direction. Interestingly, the post-growth catalyst on the top of the nanowire has a faceted morphology. Selected area electron diffraction (SAED) was used to determine the crystal structure of the catalyst, and Fig. 2(c) is such a SAED pattern taken from the catalyst in Fig. 2(b) (note that the diffraction pattern of the nanowire section was also included in the SAED pattern). Using the diffraction spots of the nanowire section as a reference (note that the lattice parameters of wurtzite structured InAs are known: $a = 0.427$ nm and $c = 0.703$ nm),[24] the lattice spacing(s) of diffraction spots of the catalyst can be determined. Our detailed SAED analysis indicates that the faceted catalyst is the hexagonal-close-packed structured Au-In ξ phase with lattice parameters of $a = 0.290$ nm and $c = 0.478$ nm.[25] To confirm the composition of the catalyst and its underling nanowire, EDS analysis was performed and results are shown in Fig. 2(d), in which the catalyst contains Au and In. Our quantitative analysis of the EDS results indicates that the nanowire is indeed InAs, and the composition of the catalyst is ~16 at. % In and ~84 at. % Au, the latter is in excellent agreement with the composition of the Au-In ξ phase (note that the solubility range of Au-In ξ phase is between ~13 at. % In and ~21 at. % In at a temperature of 430 °C). Figure 2(e) is a typical high-resolution TEM image taken from the middle of the nanowire shown in Fig. 2(a), from which many planer defects can be witnessed. To confirm these structural characteristics of the catalysts and their underlying nanowires, we have examined over a dozen of thick nanowires (all with their diameters being ~40 nm or thicker), in which faceted catalysts were confirmed in all cases.

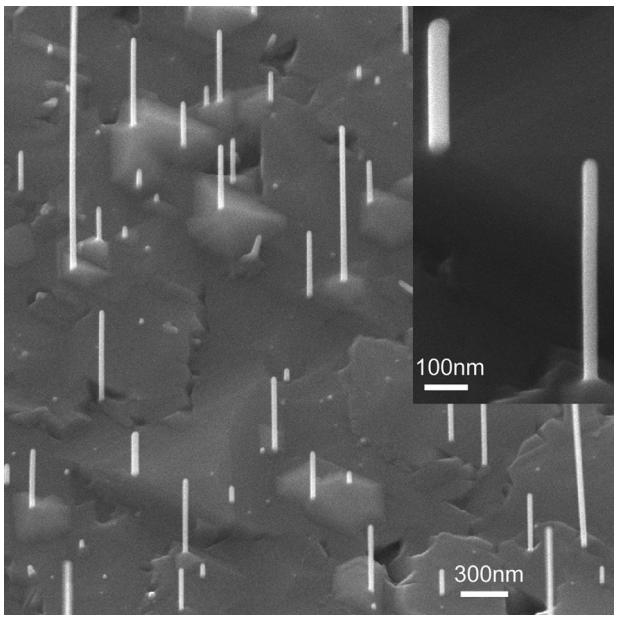

FIG. 1. SEM image showing Au-catalyzed one-dimensional InAs nanowires. The inset is a magnified image of two nanowires with different diameters.

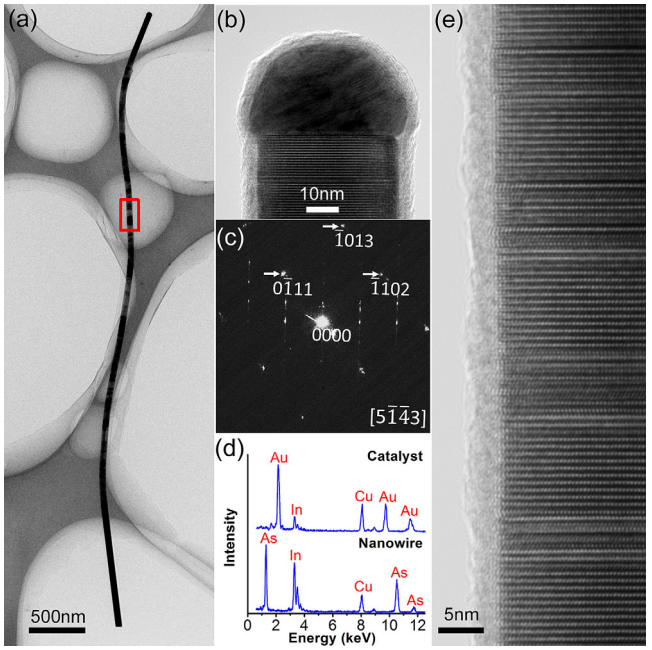

FIG. 2. TEM images of a thick InAs nanowire with a faceted catalyst. (a) A bright-field TEM image. (b) Nanowire top section with the faceted catalyst. (c) SAED pattern taken from the top of the nanowire and catalyst. (d) EDS spectra taken from the faceted catalyst and its underlying nanowire. (e) A typical high-resolution TEM image taken from the middle of InAs nanowire from marked region in (a).

Similar TEM investigations were performed on thin nanowires. Figure 3(a) shows a TEM image of a typical thin nanowire with a constant diameter of ~30 nm along the nanowire. Figure 3(b) is a high-resolution TEM image of the nanowire near the catalyst. Different to the thick nanowires, the thin nanowire has hemisphere shaped catalyst on its top. SAED was also used to determine the crystal structure of the hemisphere shaped catalyst, as shown in Fig. 3(c), in which the superimposed SAED pattern of the catalyst and its underlying nanowire was taken from the area shown in Fig. 3(b). Our detailed SAED analysis indicates that the hemisphere shaped catalyst is the hexagonal structured Au-In ϕ phase with lattice parameters of $a = 0.456$ nm and $c = 0.907$ nm (PDF 26-0710). To confirm the composition of the catalyst and its underlying nanowire, EDS analysis was performed and results are shown in Fig. 3(d), in which the nanowire contains In and As and the catalyst contains Au and In. The quantitative analysis of the EDS profiles indicates that the thin nanowire is InAs and the catalyst has a chemical composition ~39 at. % In and ~61 at. % Au. This EDS result is consistent with the composition of the Au-In ϕ phase. Figure 3(e) shows a typical high-resolution TEM image taken from middle of

This article is copyrighted as indicated in the article. Reuse of AIP content is subject to the terms at: http://scitation.aip.org/termsconditions. Downloaded to IP: 130.56.107.194 On: Fri, 04 Apr 2014 13:51:33

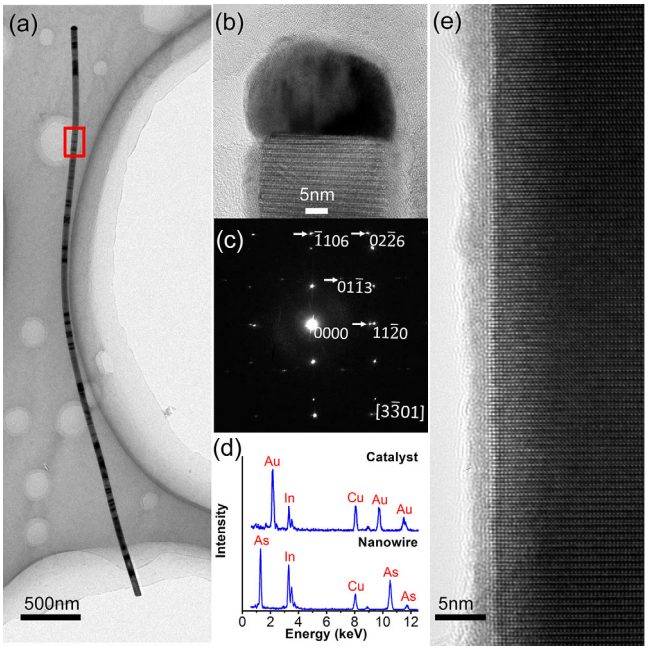

FIG. 3. TEM images of a thin InAs nanowire with a hemisphere shaped catalyst. (a) A bright-field TEM image. (b) Nanowire top section with the hemisphere shaped catalyst. (c) SAED pattern taken from the top of the nanowire and catalyst. (d) EDS spectra taken from the catalyst and its underlying nanowire. (e) A typical high-resolution TEM image taken at the middle of nanowire, marked in (a).

the nanowire shown in Fig. 3(a), in which defect-free wurtzite structured nanowire can be seen. By examining the structural quality of the entire nanowire for a dozen of thin nanowires (all with the nanowire diameters of ~30 nm or thinner), we found that all examined nanowires have the defect-free wurtzite structure and their catalysts have the hemisphere shape.

Based on our detailed characterization, we found that the smaller catalysts induce defect-free thin InAs nanowires, while larger catalysts induce defected thick InAs nanowires. To understand these findings, two questions needed to be addressed. (1) Why different sizes of catalysts result in the catalysts having different In compositions? and (2) Why smaller catalysts induce defect-free InAs nanowires and why larger catalysts induce defected InAs nanowires?

To address the first question, we need to first make sure no nanowire growth after the *formal* nanowire growth procedure (often referred as *necking*, e.g., Ref. 26 formed during the cooling stage), so that the determined chemical compositions of catalysts in the grown nanowires reflect the *true* chemical compositions during the nanowire growth. Since *necking* adopts the zinc-blende structure,[20,27] it can be clearly distinguished if the nanowires have the wurtzite dominated structure. From Figs. 2(b) and 3(b), no zinc-blende structured sections are shown, indicating no nanowire growth during the cooling stage.[28] Part of the reason is due to the strong thermodynamic affinity between Au and In,[29,30] which makes In difficult to be precipitated out from the catalysts during the cooling.[31,32] As a consequence, the measured In concentration in the post-growth catalysts should reflect to the true In concentration during the nanowire growth. Therefore, it is necessary to answer why larger catalysts contain less In than the smaller catalysts. In this regard, we believe that the In diffusion behavior in Au catalysts should play a key role in developing the ultimate In concentrations in Au catalysts. Since the surface to volume ratio increases rapidly with decreasing the catalyst size, the foreign elements should be much easier to be diffused into smaller catalysts than that into larger catalysts[33] in order to reach relatively stable concentration. Under this circumstance, for smaller catalysts, the fast In diffusion in smaller Au catalyst will lead to a high In concentration, reflecting that this is a kinetically dominated process.

To address the second question, we note two factors. (1) Theoretical calculations[15] predicted that wurtzite structure is stable in thin nanowires while zinc-blende structure is stable in thick nanowires because the total system energy of thin nanowires with the wurtzite structure is lower than those with zinc-blende structure, while the total system energy of thick nanowires shows an opposite case. (2) The In solubility in Au depends upon the nanoparticle sizes, that is, with decreasing the Au nanoparticle size, the In solubility in Au is significantly increased.[34,35] Therefore, it is anticipated that a Au catalyst with a small size tends to absorb more In atoms from the ambient vapor and leads to a higher In supersaturation, while a Au catalyst with a larger size tends to absorb less In atoms and forms a lower In supersaturation. It is generally accepted that wurtzite nucleation is favored at the high supersaturation, while with the lower supersaturation situation, zinc-blende structure is preferred.[16,17] Taking these two factors into account, nanowires catalyzed by smaller Au catalysts with a high In supersaturation tend to have the wurtzite structure, while nanowires catalyzed by larger Au catalysts with a low In supersaturation tend to develop at least some of zinc-blende structured sections when compared with the nanowires induced by smaller Au catalysts, as proposed by Joyce *et al.*[14] Therefore, the latter leads to the formation of defected wurtzite structures.

Based on the experimental results and our analysis outlined above, a growth model of Au induced InAs nanowires in MBE can be proposed, as schematically illustrated in Fig. 4. When a thin layer of Au deposited on the GaAs $\{111\}_B$ substrate is annealed under the As-rich ambient, this thin Au film is spontaneously broken down and agglomerated into Au nanoparticles of different sizes due to the Ostwald ripening effect.[36,37] With the introduction of In source, In atoms diffuse into these nanoparticles to form Au-In alloys. As a result of the In solubility difference in Au nanoparticles with different sizes, smaller Au nanoparticles may quickly absorb more In to form Au-In catalysts with a high In concentration. While larger Au nanoparticles tend to absorb In with a relatively slow rate, so that these Au-In catalysts contain a lower In concentration. As a result, InAs nanowires induced by small catalysts with a high In supersaturation have defect-free wurtzite structure, while defected InAs nanowires are induced by larger catalysts with a low In supersaturation, as demonstrated by the high-resolution TEM images shown in Fig. 4. It should be noted that the size difference between small and large Au nanoparticles prior to the InAs nanowire growth is more significant than that after the nanowire growth, due to the fact that high In residue is found in smaller post-growth catalysts than that in larger post-growth catalysts as shown by our extensive TEM analyses.

This article is copyrighted as indicated in the article. Reuse of AIP content is subject to the terms at: http://scitation.aip.org/termsconditions. Downloaded to IP: 130.56.107.194 On: Fri, 04 Apr 2014 13:51:33

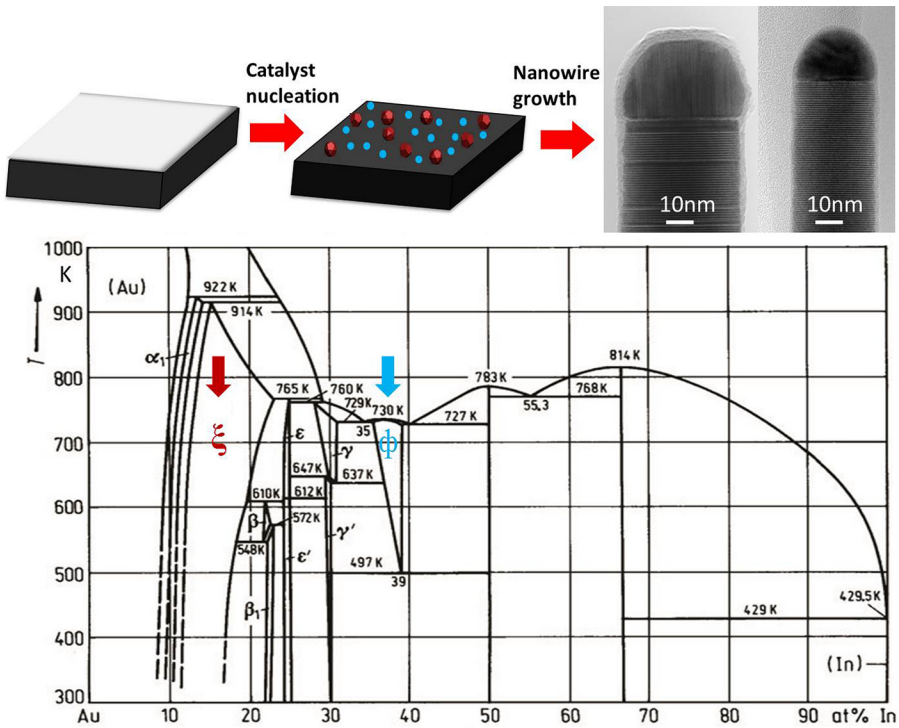

FIG. 4. Schematic illustrating the growth mechanism of InAs nanowires induced by Au catalysts with different sizes and compositions. The smaller hemisphere catalysts contain a high In concentration that induce defect-free InAs nanowires, and the larger faceted catalysts contain a low In concentration that induce defected InAs nanowires.

In conclusion, the structural quality of epitaxial InAs nanowires catalyzed by a Au thin film in MBE has been found to be dependent upon the size and composition of Au catalysts in a single growth. It was found that the original Au breakdown sizes from the Au thin film play a key role in determining the composition of the catalysts during the nanowire growth, and in turn the structural quality of grown InAs nanowires. The fact of enhanced In diffusion in smaller Au catalysts leads to the formation of high In concentrated catalysts that induce defect-free InAs nanowires, while relatively slow In diffusion in larger Au catalysts results in the formation of low In concentrated catalysts that induce defected InAs nanowires. This finding provides an insight into the realization of defect-free wurtzite InAs nanowires in MBE.

This study was financially supported by the Australian Research Council, the National Basic Research Program of China (Grant No. 2011CB925604), and the National Science Foundation of China (Grant Nos. 91021015, 10990103, and 91121009). Australian Microscopy & Microanalysis Research Facility is also gratefully acknowledged for providing microscopy facilities for this study.

[1]Y. Kim, H. J. Joyce, O. Gao, H. H. Tan, C. Jagadish, M. Paladugu, J. Zou, and A. A. Suvorova, Nano Lett. **6**, 599 (2006).
[2]H. Xia, Z. Y. Lu, T. X. Li, P. Parkinson, Z. M. Liao, F. H. Liu, W. Lu, W. D. Hu, P. P. Chen, H. Y. Xu, J. Zou, and C. Jagadish, ACS Nano **6**, 6005 (2012).
[3]R. S. Wagner and W. C. Ellis, Appl. Phys. Lett. **4**, 89 (1964).
[4]O. Moutanabbir, D. Isheim, H. Blumtritt, S. Senz, E. Pippel, and D. N. Seidman, Nature **496**, 78 (2013).
[5]H. D. Park, A. Gaillot, S. M. Prokes, and R. C. Cammarata, J. Cryst. Growth **296**, 159 (2006).
[6]S. A. Dayeh, D. P. R. Aplin, X. Zhou, P. K. L. Yu, E. T. Yu, and D. Wang, Small **3**, 326 (2007).
[7]S. L. Wright, R. F. Marks, S. Tiwari, T. N. Jackson, and H. Baratte, Appl. Phys. Lett. **49**, 1545 (1986).
[8]A. G. Milnes and A. Y. Polyakov, Mater. Sci. Eng., B **18**, 237 (1993).
[9]C. Thelander, T. Martensson, M. T. Bjork, B. J. Ohlsson, M. W. Larsson, L. R. Wallenberg, and L. Samuelson, Appl. Phys. Lett. **83**, 2052 (2003).
[10]Y. J. Doh, J. A. van Dam, A. L. Roest, E. Bakkers, L. P. Kouwenhoven, and S. De Franceschi, Science **309**, 272 (2005).
[11]M. T. Bjork, B. J. Ohlsson, C. Thelander, A. I. Persson, K. Deppert, L. R. Wallenberg, and L. Samuelson, Appl. Phys. Lett. **81**, 4458 (2002).
[12]X. Zhou, S. A. Dayeh, D. Aplin, D. Wang, and E. T. Yu, Appl. Phys. Lett. **89**, 053113 (2006).
[13]S. Chuang, Q. Gao, R. Kapadia, A. C. Ford, J. Guo, and A. Javey, Nano Lett. **13**, 555 (2013).
[14]H. J. Joyce, J. Wong-Leung, Q. Gao, H. H. Tan, and C. Jagadish, Nano Lett. **10**, 908 (2010).
[15]T. Akiyama, K. Sano, K. Nakamura, and T. Ito, Jpn. J. Appl. Phys., Part 2 **45**, L275 (2006).
[16]F. Glas, J.-C. Harmand, and G. Patriarche, Phys. Rev. Lett. **99**, 146101 (2007).
[17]V. G. Dubrovskii, N. V. Sibirev, J. C. Harmand, and F. Glas, Phys. Rev. B **78**, 235301 (2008).
[18]J. Johansson, K. A. Dick, P. Caroff, M. E. Messing, J. Bolinsson, K. Deppert, and L. Samuelson, J. Phys. Chem. C **114**, 3837 (2010).
[19]H. Y. Xu, Y. N. Guo, Z. M. Liao, W. Sun, Q. Gao, H. H. Tan, C. Jagadish, and J. Zou, Appl. Phys. Lett. **102**, 203108 (2013).
[20]J. C. Harmand, G. Patriarche, N. Pere-Laperne, M. N. Merat-Combes, L. Travers, and F. Glas, Appl. Phys. Lett. **87**, 203101 (2005).
[21]H. Y. Xu, Y. Wang, Y. N. Guo, Z. M. Liao, Q. Gao, N. Jiang, H. H. Tan, C. Jagadish, and J. Zou, Cryst. Growth Des. **12**, 2018 (2012).
[22]X. Zhang, J. Zou, M. Paladugu, Y. N. Guo, Y. Wang, Y. Kim, H. J. Joyce, Q. Gao, H. H. Tan, and C. Jagadish, Small **5**, 366 (2009).
[23]J. Zou, M. Paladugu, H. Wang, G. J. Auchterlonie, Y. N. Guo, Y. Kim, Q. Gao, H. J. Joyce, H. H. Tan, and C. Jagadish, Small **3**, 389 (2007).
[24]D. Kriegner, C. Panse, B. Mandl, K. A. Dick, M. Keplinger, J. M. Persson, P. Caroff, D. Ercolani, L. Sorba, F. Bechstedt, J. Stangl, and G. Bauer, Nano Lett. **11**, 1483 (2011).
[25]S. E. R. Hiscocks and W. Hume-Rothery, Proc. R. Soc. London, Ser. A **282**, 318 (1964).
[26]H. Y. Xu, Y. Wang, Y. N. Guo, Z. M. Liao, Q. Gao, H. H. Tan, C. Jagadish, and J. Zou, Nano Lett. **12**, 5744 (2012).
[27]A. I. Persson, M. W. Larsson, S. Stenstrom, B. J. Ohlsson, L. Samuelson, and L. R. Wallenberg, Nature Mater. **3**, 677 (2004).
[28]H. D. Park, S. M. Prokes, and R. C. Cammarata, Appl. Phys. Lett. **87**, 063110 (2005).
[29]B. M. Borg, K. A. Dick, B. Ganjipour, M. Pistol, L. Wernersson, and C. Thelander, Nano Lett. **10**, 4080 (2010).

This article is copyrighted as indicated in the article. Reuse of AIP content is subject to the terms at: http://scitation.aip.org/termsconditions. Downloaded to IP: 130.56.107.194 On: Fri, 04 Apr 2014 13:51:33

[30]Y. N. Guo, H. Y. Xu, G. Auchterlonie, T. Burgess, H. J. Joyce, Q. Gao, H. H. Tan, C. Jagadish, H. B. Shu, X. S. Chen, W. Lu, Y. Kim, and J. Zou, Nano Lett. **13**, 643 (2013).
[31]M. Paladugu, J. Zou, Y. N. Guo, G. Auchterlonie, H. J. Joyce, Q. Gao, H. H. Tan, C. Jagadish, and Y. Kim, Small **3**, 1873 (2007).
[32]M. Paladugu, J. Zou, Y. N. Guo, X. Zhang, Y. Kim, H. J. Joyce, Q.Gao, H. H. Tan, and C. Jagadish, Appl. Phys. Lett. **93**, 101911 (2008).
[33]A. K. Sra and R. E. Schaak, J. Am. Chem. Soc. **126**, 6667 (2004).
[34]G. Q. Zhang, K. Tateno, H. Sanada, T. Tawara, H. Gotoh, and H. Nakano, Appl. Phys. Lett. **95**, 123104 (2009).
[35]N. Han, F. Y. Wang, J. J. Hou, S. Yip, H. Lin, M. Fang, F. Xiu, X. L. Shi, T. Hung, and J. C. Ho, Cryst. Growth Des. **12**, 6243 (2012).
[36]H. Y. Xu, Y. N. Guo, W. Sun, Z. M. Liao, T. Burgess, H. F. Lu, Q. Gao, H. H. Tan, C. Jagadish, and J. Zou, Nanoscale Res. Lett. **7**, 589 (2012).
[37]P. W. Voorhees, J. Stat. Phys. **38**, 231 (1985).

This article is copyrighted as indicated in the article. Reuse of AIP content is subject to the terms at: http://scitation.aip.org/termsconditions. Downloaded to IP: 130.56.107.194 On: Fri, 04 Apr 2014 13:51:33